

Mass Extinctions and The Sun's Encounters with Spiral Arms

Erik M. Leitch & Gautam Vasisht
California Institute of Technology, 105-24
Pasadena CA 91125

ABSTRACT

The terrestrial fossil record shows that the exponential rise in biodiversity since the Precambrian period has been punctuated by large extinctions, at intervals of 40 to 140 Myr. These mass extinctions represent extremes over a background of smaller events and the natural process of species extinction. We point out that the non-terrestrial phenomena proposed to explain these events, such as boloidal impacts (a candidate for the end-Cretaceous extinction), and nearby supernovae, are collectively far more effective during the solar system's traversal of spiral arms. Using the best available data on the location and kinematics of the Galactic spiral structure (including distance scale and kinematic uncertainties), we present evidence that arm crossings provide a viable explanation for the timing of the large extinctions.

The literature is replete with suggestions of non-terrestrial phenomena as the candidate causes for large scale extinctions. The most frequently invoked are supernovae and boloidal impacts (e.g. comets from the Oort Cloud), the latter a strong candidate for the K/T extinction ever since the discovery of the Iridium anomaly in the K/T boundary clay (Alvarez et al. 1990). Certainly the most violent events in the solar neighborhood during geologic history would have been supernovae (barring the possibility of a nearby γ -ray burst, which is far less likely; Thorsett 1995); that the structure of the very local interstellar medium is considered to be the result of a supernova, possibly related to the Geminga pulsar (at 150 pc) (Bignami & Caraveo 1996), is an impressive reminder of their potential impact. Supernovae and young supernova remnants, especially those occurring at distances $\lesssim 10$ pc (Ruderman 1974), can result in biospheric imbalance through a variety of processes, including ozone depletion by enhanced ionizing radiation and cosmic rays (Ellis & Schramm 1995, Koyama et al. 1995), the absorption of visible light by the formation of NO_2 (Crutzen & Brühl 1996), and in rare cases the direct deposition of supernova debris.

Tidal and collisional encounters with intermediate-sized gas or dust clouds might focus cometary activity ($\sim 10^9$ comets) to the inner solar system, by scattering of Oort Cloud member bodies, a mechanism proposed to explain the K/T boundary event. In addition, the passage of the Sun through a cloud of density $n \gtrsim 10^4 \text{ cm}^{-3}$ could raise the solar luminosity significantly, through Bondi accretion, as well as raise the opacity of Earth's atmosphere, directly affecting the insolation on Earth (McCrea 1975). While the recent association of the Chicxulub crater with the K/T boundary lends credence to the boloidal impact model, the large concentration of Ir deposited at the boundary may indicate that accretion also played an important role (Yabushita & Allen 1997).

The proposed mechanisms constitute a set of plausible external agents for any one extinction, yet do not of themselves suggest any explanation for the timing of the mass extinctions, or for the large variation in severity of the observed extinctions. Hatfield and Camp (1970) were among the first to suggest that extinctions might be correlated with Galactic-plane crossing due to the solar orbit's vertical oscillations. Rampino and Stothers (1984), as well as Schwartz and James (1984), have invoked these z-oscillations in connection with the suggested $\sim 26 - 30$ Myr periodicity of minor extinctions, as virtually all of the postulated extinction mechanisms concentrate toward the Galactic plane. However, the fact that we

are presently half-way between extinction cycles and that the Sun’s position is nearly midplane implies that Galactic plane passages are unlikely causes for the extinctions, unless the Sun has suffered a violent gravitational encounter in the last 15 Myr (Clube & Napier 1996). Moreover, even if the correlation were exact, it does not explain the enormous difference in magnitude between the 6 largest extinctions and extinctions which occur on 30 Myr timescales.

While acknowledging that the apparent quasi-periodicity of mass extinctions may in fact be spurious, and that the extinction record may be one of chance encounters of varying magnitude, or indeed merely a record of terrestrial cataclysms, we suggest that the spiral arm environment of the Galaxy provides a natural framework in which all of the astrophysical mechanisms discussed thus far would operate most efficiently. Pre-supernova stars (the luminous O and B stars) are born primarily in the spiral arms, and spend much of their short lifetimes ($\lesssim 2 \times 10^7$ yr) in their vicinity. The Type II/Ib supernovae, which are a consequence of the core-collapse of OB stars, have a Galactic rate of roughly $R_{SN} \approx 1/30 \text{ yr}^{-1}$ (van den Bergh & Tamman 1991) and are distributed with a scale height $z \simeq 10^2$ pc in the disk. The longest lifetime of a pre-supernova star is $\tau \simeq 2 \times 10^7$ yr (for masses $M \gtrsim 8 - 9 M_\odot$). Defining the effective distance over which a supernova may have a profound impact on the biosphere as $l_k \simeq 10$ pc (Ellis & Schramm 1995), the number of significant supernova encounters at the solar Galactic radius is $N_{SN} \simeq R_{SN} l_k^3 \tau / N_{sp} A_{sp} z$, where $N_{sp} \simeq 4$ is the number of Galactic arms. The influence area A_{sp} is assumed to be roughly the product of the arm-length ~ 10 kpc and the arm-width, i.e. $(\Omega_\odot - \Omega_p) R_0 \tau$, where Ω_\odot is the angular speed at the solar galactocentric radius, Ω_p is the pattern speed of the spiral arms (see below) and $\tau \sim 10^7$ is the average lifetime of a supernova progenitor star. Then,

$$N_{SN} \simeq 0.5 \left(\frac{R_{SN}}{0.033 \text{ yr}^{-1}} \right) \left(\frac{l}{10 \text{ pc}} \right)^3 \left(\frac{\tau}{10^7 \text{ yr}} \right) \left(\frac{z}{100 \text{ pc}} \right)^{-1} \left(\frac{A_{sp}}{6 \text{ kpc}^2} \right)^{-1} \left(\frac{N_{sp}}{4} \right)^{-1}$$

is the typical number of supernovae encountered within l_k during one spiral arm passage. In addition, recent X-ray observations have shown that young supernova remnants (of radius $\lesssim 10$ pc) are active sites of acceleration of cosmic rays to energies $\gtrsim 10^2$ TeV (Koyama et al. 1995). The above estimate shows that the chances of intercepting a supernova shock front are significant, leading to sustained exposure ($\sim 10^4$ yr) of the upper atmosphere to cosmic ray bombardment, by factors $10^2 - 10^3$ over the mean level.

Besides supernovae, gravitational perturbers such as large complexes of molecular gas and dust (the giant molecular clouds and the intermediate sized clouds), with typical sizes of a few hundred parsecs and masses of up to $10^6 M_\odot$, are also concentrated along spiral arms. It is instructive, therefore, to trace the first order solar orbit through the best estimate of the structure of the Milky Way and the position of its spiral arms, back to the beginning of the Phanerozoic period (0 – 500 Myr-ago, or $\lesssim 5\%$ of the age of the Galactic disk). Episodes during the solar motion may then be compared directly with episodes in the geologic timeline.

In its simplest approximation, the solar revolution is circular with an adopted galactocentric radius $R_0 \simeq 8.5$ kpc. Radial and vertical oscillations may be considered small departures from an otherwise circular orbit (e.g. the vertical oscillation has a period $P \simeq 62$ Myr and amplitude ~ 35 pc (Binney & Tremaine 1987), smaller than the scale heights of the perturber populations). Severe gravitational encounters are unlikely to have distorted this orbit over the past 0.5 Gyr (i.e. two dynamical times) making it reasonable to assume that the Sun has preserved its nearly circular motion, with angular speed $\Omega_\odot \simeq 27 \text{ km s}^{-1} \text{ kpc}^{-1}$ ($v_\odot \simeq 230 \text{ km s}^{-1}$).

The spiral density waves trail the disk rotation with a characteristic pattern speed $\Omega_p \simeq 19 \pm 5 \text{ km s}^{-1} \text{ kpc}^{-1}$ (Wada et al. 1994), implying that the solar system streams through the arms at a mean

relative speed $v_r \simeq 68 \text{ km s}^{-1}$. Due to the inherent difficulty of the measurement, the pattern speed is not an accurately determined quantity and contributes the largest uncertainties to any estimate of the past structure of the Galaxy. Methods for estimating Ω_p have included measurement of the age gradient of objects along the Sagittarius-Carina arm (Avedisova 1989) and the velocity field of Cepheids (Mishurov et al. 1979). Amaral and Lépine (1997) estimated Ω_p based on a study of open clusters, an ideal population for such a study since their ages are well determined from the HR diagram. Their analysis suggests that $\Omega_p \simeq 20 \pm 5 \text{ km s}^{-1} \text{ kpc}^{-1}$. The estimate derived by Wada et al. (1994) is for the pattern speed of a putative end-on Galactic bar based on modeling of the molecular cloud longitude-velocity diagram. Other arguments have been summarized by Amaral (1995) in favor of $\Omega_p \simeq 20 \text{ km s}^{-1} \text{ kpc}^{-1}$.

The present day positions of the spiral arms have been outlined using optical and radio observations of large H II regions (Georgelin & Georgelin 1976), supplemented by data from the 21-cm line of neutral hydrogen, the H109 α radio recombination line, and the 2.6-mm line of carbon monoxide (which traces molecular hydrogen), used to resolve distance ambiguities. The highly excited H II regions define two pairs of arms (four major arms altogether), which intersect the solar orbit at angles of 10° – 12° . The face-on morphology of the Galaxy is shown in Figure 1, along with the location of the Sun during each of the six Phanerozoic extinctions. The data for the major arm (the Sagittarius-Carina arm) and the intermediate arm (the Scutum-Crux arm) are complete out to the solar galactocentric radius of 8.5 kpc. However, data is unavailable for the internal arm (the Norma arm) beyond a galactocentric radius of $\simeq 6.0$ kpc, due to obscuration by the Galactic center. We extend this arm to the solar orbital radius using a logarithmic spiral model (Avedisova 1996); this function provides excellent corroborating fits to arms for which data do exist.

Figure 2 displays the times of solar spiral arm crossings in graphical form (assuming a relative speed of 68 km s^{-1}) through the Galactic free-electron distribution, as modeled by Taylor and Cordes (1993), based on the radio and optical data of giant H II regions and corroborated by γ -ray observations of Al-26, a tracer of massive star nucleosynthesis (Chen et al. 1996). The free electron density (or equivalently the ionized gas density) is a tracer of spiral structure; ionized gas in the Galaxy is concentrated in the H II regions surrounding hot OB stars, young star clusters, and in the near exteriors and interiors of expanding supernova remnants. Dotted lines indicate the range of uncertainty in the past positions of the spiral arms due to unwinding. (A simple way to estimate the unwinding is to notice that the phase winding between the innermost regions of the arms (the so-called inner Lindblad resonance where $\Omega_d \approx 0 \text{ km s}^{-1} \text{ kpc}^{-1}$ and $R \simeq 4.0$ kpc) to those at radius R_0 is $\simeq \pi$ rad (Figure 1), over a time roughly equal to the age of the Galactic disk $\simeq 12$ Gyr. The phase unwinding for individual crossings is then $\sim 1^\circ$, $\sim 4^\circ$ and $\sim 8^\circ$, respectively, for the first three spiral arms. A more detailed calculation gives 2.4° , 10° and 20° ; Binney & Tremaine 1987).

Along with the crossing times, Figure 2 illustrates the extinction timeline adopted from Sepkoski (1994), where individual extinctions are modeled as gaussians after the subtraction of a mean background extinction rate at each epoch. Notice a correlation between the two timeseries, which *a priori* represent two rather disparate temporal sequences, i.e., the solar spiral arm crossing times and the geological times of terrestrial extinction. Perhaps most interesting, as it involves the smallest extrapolation in time, is the close coincidence of the K/T (Maastrichtian) event with the Sagittarius-Carina arm crossing 60 Myr-ago (0.6 % the disk age) for the above-mentioned kinematic parameters. Further back in time, the end-Permian and upper Norian events coincide with the crossing of the Scutum-Crux arm. The upper Botomian and possibly the late Ordovician (Ashgillian) extinctions may be associated with the Norma arm, but the large uncertainty in the position of this arm makes any definite association specious at best. The late Devonian (Frasnian) extinction does not coincide with any major arm, although a detailed statistical examination

(Hubbard & Gilinsky 1993) of the extinction record suggests that the Devonian and Norian events should only be regarded as candidates for extinctions. It is well worth mentioning that independent of our assumed distance scale and kinematic model, the ratios of timescales in the geologic record are a good match to those of the three spiral crossings (assuming an unperturbed solar orbit).

The uncertainties involved in the above analysis are admittedly quite large, and any quantitative comparison should naturally be regarded with caution. Yet in the face of the terrestrial geologic record, and the near certainty that at least one of the mass extinctions is linked to non-terrestrial mechanisms, we find an idea which unifies these mechanisms appealing. If a fraction of mass extinctions are indeed due to non-terrestrial phenomena, then the concentration of supernovae and other perturbers ought to make spiral arms far more hazardous than other locations in the Galaxy. A comparison between the extinction record and the best available data on the spiral structure of the Galaxy suggests that this may indeed be the case; although the large uncertainties in the spiral arm pattern speed, as well as the locations of the arms themselves prevent a more definitive comparison, it is nonetheless intriguing that the observed spacing of the major extinctions is approximately reproduced. Moreover, evidence from the fossil record (Officer et al 1987) (and possibly the Ir evidence; Yabushita & Allen 1997) that the mass extinctions were far more gradual than previously thought, lends credence to the spiral arm hypothesis, as the Sun spends tens of Myr in the vicinity of each arm, during which any or all of the aforementioned processes are not only possible, but likely. If both boloidal impacts (the Iridium evidence) and supernovae are established as culprits-in-common (as per the suggestions of Ellis, Fields and Schramm 1996) from either geological or ice-layer records, then spiral arm crossing must play an important role in the repeated extinction of terrestrial (or extra-terrestrial) life.

Acknowledgments: We thank J. H. Taylor and J. M. Cordes for making their Galactic free-electron density model widely available, as this paper makes use of their software. We thank T. Padmanabhan, A. C. S. Readhead, M. R. Metzger and S. R. Kulkarni for several useful discussions.

REFERENCES

- Amaral, L. H. 1995, PhD Thesis, Univ. São Paulo, Instituto Astronômico e Geofísico
- Amaral, L. H. & Lépine, J. R. D. 1997, MNRAS, 286, 885.
- Alvarez, W., Asaro, F., & Montanari, A., 1990, Science, 250, 1700-1702.
- Alvarez, W. & Muller, R. A., 1984, Nature, 308, 718-720.
- Avedisova, V. S. 1989, Astrophys., Vol 30, No. 1, 83.
- Avedisova, V. S., 1996, Astronomy Letters, 22, 443-454: Translated from Pisma v Astronomicheskii Zhurnal, 1996, 22, No., 7-8.
- Bignami, G. F. & Caraveo, P. A., 1996, ARAA, 34, 331-381.
- Binney, J. & Tremaine, S., 1987, Galactic Dynamics, Princeton Univ. Press, 350.
- Chen, W., Gehrels, N., Diehl, R., & Hartmann, D., A&AS, 1996, 120, 315-316.
- Clube, S. V. M. & Napier, W. M., 1996, QJRAS, 37, 617-642.
- Crutzen, P. J. & Brühl, C., 1996, PNAS, 93, 1582-1584.
- Ellis, J. & Schramm, D. N., 1995, PNAS, 92, 235-238.
- Ellis, J., Fields, B. D., Schramm, D. N., 1996, ApJ, 470, 1227-1236.
- Georgelin, Y. M. & Georgelin, Y. P., 1976, A&A, 49, 57-59.
- Hatfield, C. B. & Camp, M. J., 1970, Bull. geol. Soc. Am., 81, 911-914.
- Hubbard, A. E. & Gilinsky, N. L. 1993, 1992, Paleobiology, 18, 148-160.
- Koyama, K., Petre, R., Gotthelf, E. V., Hwang, U., Matsuura, M., Ozaki, M. & Holt, S. S., 1995, Nature, 378, 255-258.
- McCrea, W. H., 1975, Nature, 255, 607-609.
- Mishurov, Y. N., Pavlovskaya, E. D., Suchkov, A. A. 1979, AZh, 56, 286.
- Officer, C. B., Hallam, A. D., Drake, C. L. & Devine, J. D., 1987, Nature, 326, 143-149.
- Rampino, M. R. & Stothers, R. B., 1984, Nature, 308, 709-711.
- Rampino, M. R. & Haggerty, B. M., 1996, Earth Moon & Planets, 72, 441-460.
- Raup, D. M. & Sepkoski, J. J. Jr, 1982, Science, 25, 1501-1503.
- Raup, D. M., 1991, Paleobiology, 17, 37-48.
- Ruderman, M. A., 1974, Science, 184, 1079-1081.
- Sepkoski, J. J., 1994, Geotimes, March 1994, 15-1.
- Schwartz, R. D. & James, P. B., 1984, Nature, 308, 712-713.
- Taylor, J. H. & Cordes, J. M., 1993, ApJ, 411, 674-684.
- Thorsett, S. E., ApJ, 1995, 444, L53-L55.
- van den Bergh, S. & Tammann, G. 1991, 1991, ARAA, 29, 363-407.
- Wada, K., Taniguchi, Y., Habe, A. and Hasegawa, T., 1994, ApJ, 437, L123.
- Yabushita, S. & Allen, A., 1997, Astronomy & Geophysics, 38 (2), 15.

1. APPENDIX

In this appendix, we present a somewhat more detailed comparison of the two timeseries shown in Figure 2. Mass extinctions are identified as in Sepkoski (1994). As described in the text, the individual extinctions are modeled as gaussians after subtraction of a mean extinction rate at each epoch, estimated from the troughs in the extinction record. We find that the cross-correlation of the two time series peaks at $\Delta t = 0$ for a relative velocity of $v_s = 68.4$ km/s (the expected value for $\Omega_p \approx 19$ km s⁻¹ kpc⁻¹).

The statistical significance of the observed cross-correlation is assessed using Monte Carlo methods. The locations of the individual extinctions are uniformly randomized within the time bounds of the Phanerozoic period. Two preconditions are applied when generating the fake datasets: (i) the individual extinctions are not allowed to overlap each-other within 2σ -bounds (since geological methods have to distinguish them as distinct events), and (ii) wherever model extinctions do partially overlap, their sum is truncated at the 100 percent level. In addition, we let the orbital speed of the Sun in the frame corotating with the arms (i.e. $v_s = (\Omega_p - \Omega_\odot)R_0$), be a gaussian random variable; that is, we let $\Omega_p = 19 \pm 5$ km s⁻¹ kpc⁻¹ (1σ). We generate 10^5 fake extinction datasets, and for each we compute the zero-lag cross-correlation with the spiral arm crossing curve. We find that 99 percent of the randomly generated correlations were smaller than the actual data correlation. The highest tail-end cross-correlations, when examined carefully, displayed rough positional interchange and strong clumping of the extinction gaussians around the spiral arms, as expected.

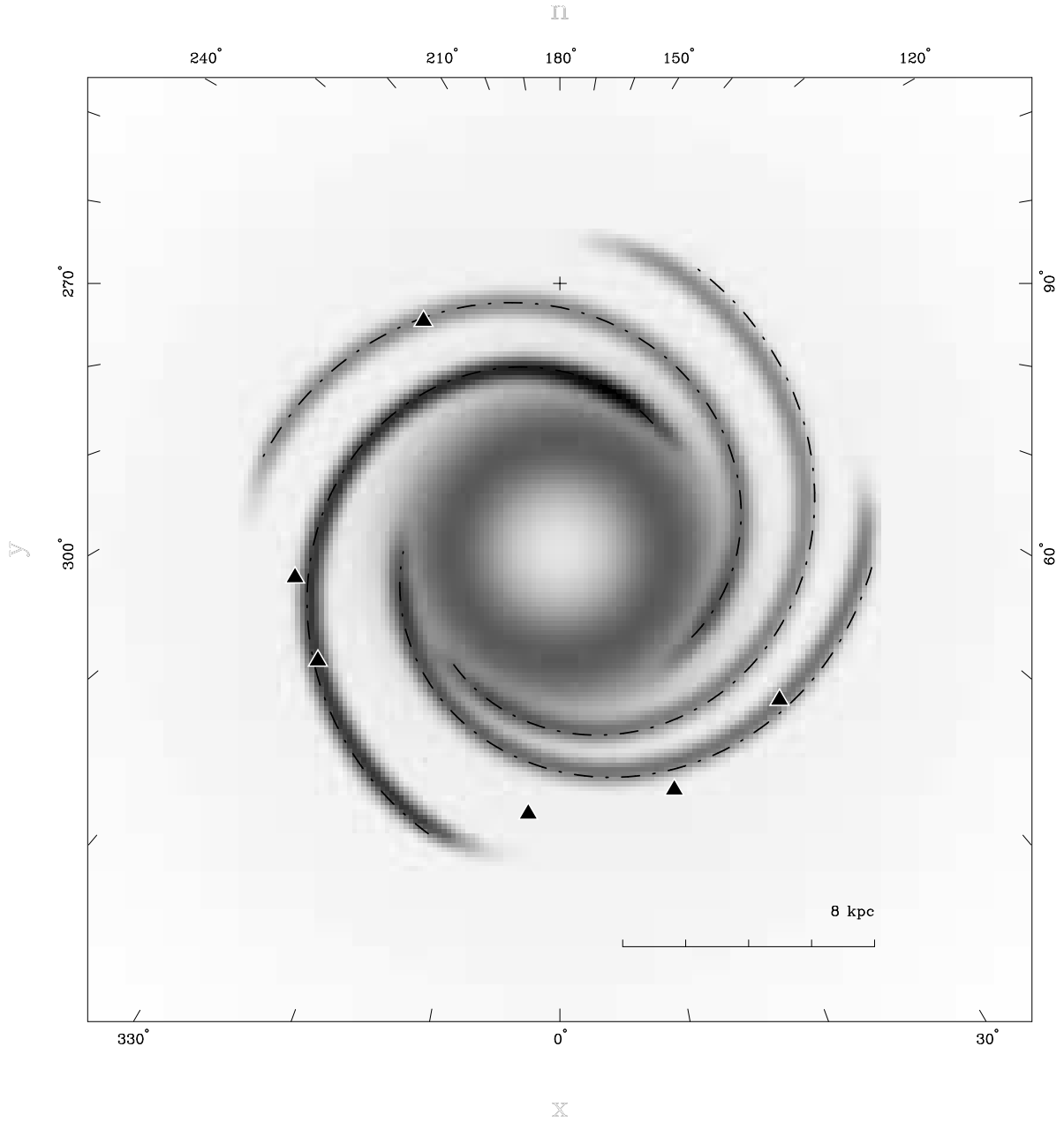


Fig. 1.— Face-on view of the Galaxy. Arms are fits of logarithmic spirals to the Taylor-Cordes model, extrapolated to $R \sim 12$ kpc, with peak densities equal to the value at the solar radius. Counterclockwise from the Sun (cross at top) are the Sagittarius-Carina, Scutum-Crux, Norma and Perseus arms. Triangles mark the times of the major terrestrial extinctions. The effect of unwinding is indicated by the dot-dashed lines defining the centroids of the arms for an unwinding of 1° , 4° and 8° for the first three arms, respectively.

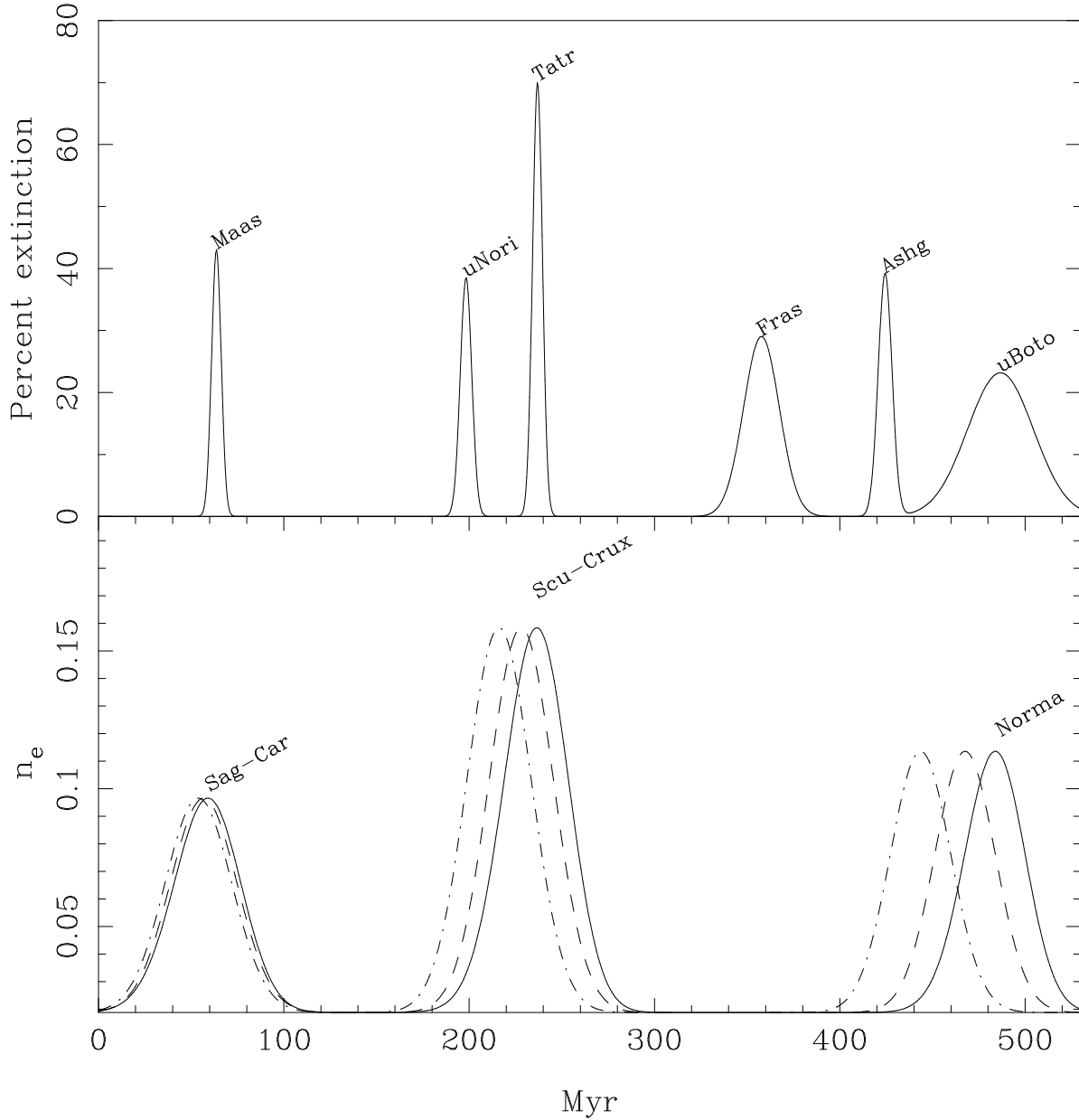


Fig. 2.— (Top panel) Gaussian fits to peak percent extinctions (after Sepkoski (1994)), after subtraction of a mean extinction level at each epoch. (Bottom panel) Spiral arm crossings (traced by electron density); locations and approximate widths of the spiral arms are taken from the model of Taylor and Cordes (1993). The Norma arm is an extrapolation to the solar galactocentric radius of a fit to the Taylor-Cordes model. The effect of unwinding is shown by the dashed line (1° , 4° and 8° for the Sagittarius- Carina, Scutum-Crux and Norma arms, respectively) and the dot-dashed line (2° , 10° and 20°).